




RESEARCH ARTICLE

Performance Evaluation of a Newly Developed MR-Compatible Mobile PET Scanner with Two Detector Layouts

Masao Watanabe,¹ Yuji Nakamoto ,¹ Ryusuke Nakamoto,² Takayoshi Ishimori,¹ Tsuneo Saga,¹ Kaori Togashi¹

¹Department of Diagnostic Imaging and Nuclear Medicine, Graduate School of Medicine, Kyoto University, 54 Shogoinawahara-cho, Sakyo-Ku, Kyoto, 606-8507, Japan

²Department of Radiology, Shiga General Hospital, 5-4-30 Moriyama, Moriyama, Shiga, 524-8524, Japan

Abstract

Purpose: A mobile positron emission tomography (PET) scanner called flexible PET (fxPET), designed to fit existing magnetic resonance imaging (MRI) or computed tomography (CT) system, has been developed. The purpose of this study was to evaluate the image quality, lesion detection rate, and quantitative values of fxPET compared with conventional bismuth germanium oxide (BGO)-based PET/CT without time-of-flight capability.

Procedures: Fifty-nine patients underwent whole-body (WB) PET/CT scans approximately 1 h after injection of 2-deoxy-2-[¹⁸F]fluoro-D-glucose, followed by the fxPET scans with detectors located above and below the patients (layout A) and with detectors closer to the patients (layout B). Two readers assessed the image quality using a 4-point grade for each layout and reached a consensus. We evaluated the differences and/or correlations between fxPET and WB PET/CT, including the lesion detection rates, the standardized uptake value (SUV), the metabolic tumor volume (MTV), the total lesion glycolysis (TLG), the tumor-to-normal liver ratio (TLR), and the background liver signal-to-noise ratio (SNR).

Results: The image quality of layout B was better than layout A ($p < 0.0001$). Of 184 lesions, the detection rate of layout B was significantly higher than WB PET/CT ($p = 0.041$), while the detection rate of layout A was comparable to WB PET/CT. The SUV_{max}/mean/peak were larger, and the MTVs were smaller in fxPET than WB PET/CT, especially in the lesions smaller than 2 cm ($p < 0.01$). The SUV_{max}/mean/peak, the MTVs and the TLGs of fxPET had significant positive correlations with WB PET/CT ($p < 0.0001$). The TLRs were significantly larger ($p < 0.0001$), but the background SNRs were significantly lower in fxPET than WB PET/CT ($p < 0.05$).

Conclusions: The fxPET system yielded reasonable image quality and quantitative accuracy. Bringing the detectors closer to the patient yielded improved results.

Key Words: Mobile flexible PET, Detection rate, Image quality, Standardized uptake value (SUV), Tumor-to-liver ratio (TLR), Background signal-to-noise ratio (SNR)

This article was updated to correct the “greater than or equal to” (\geq) symbols in Tables 4 and 5, which incorrectly appeared as “greater than” ($>$) symbols. Electronic supplementary material The online version of this article (<https://doi.org/10.1007/s11307-019-01384-9>) contains supplementary material, which is available to authorized users.

Correspondence to: Yuji Nakamoto; e-mail: ynakamo1@kuhp.kyoto-u.ac.jp

Published online: 20 June 2019

Introduction

Positron emission tomography (PET)/computed tomography (CT) scanners are widely used in clinical oncology. Currently, a combined PET/magnetic resonance (MR) imaging scanner is

also used, which allows clinicians to obtain higher tissue contrast using MR as a part of PET/MR [1]. Additionally, the PET/MR scanner enables clinicians to reduce redundant radiation exposure compared with PET/CT [1], especially in repeated examinations after treatment. The advantage of MR over CT is especially evident in the brain, head-and-neck, liver, prostate, and bone [1]. However, PET/MR is expensive and is not always affordable in every institute.

A newly developed flexible mobile PET scanner (fxPET) is an MR-compatible PET scanner designed to fit existing MR systems, which allows clinicians to obtain accurate fused images from PET and existing MR with minimum misalignment [2]. The characteristics of our fxPET scanner are discussed in the literature, with a focus on count recovery, time-of-flight (TOF), spatial resolution, and misalignment between fxPET images and existing MR images [2–6]. In this system, detectors are typically located above and below the patient (layout A, Fig. 1a) with no detectors to either side of the patient. In a previous phantom study, the performance of layout A was better than that of the layout with two detectors lateral to the phantom [3]. However, image quality may be suboptimal because of the incomplete partial-ring detectors. To eliminate the gap of detectors, we can move detectors closer to patients (layout B, Fig. 1b). However, it remains unknown if this would really improve the image quality and lesion detection rate and how different the quantitative values are in each layout.

The purpose of this study was to investigate the image quality, the lesion detectability, and the difference and correlation of quantitative values including maximum standardized uptake value (SUVmax) between the two fxPET layouts and whole-body (WB) PET/CT.

Materials and Methods

Patients

The study protocol was approved by the institutional review board with the research protocol number C1163 and was registered by University Hospital Medical Information Network (UMIN) with the ID number UMIN000022196.

Between August 2016 and January 2017, 59 consecutive patients with known or suspected malignancy (32 male and 27 female, age 58.5 ± 13.1 years, mean \pm SD (standard deviation), range 24–79 years), who signed written informed consent, were enrolled prospectively. The disease characteristics of the patients are summarized in Table 1.

Flexible PET Scanner System

The precise mechanical information of fxPET was described in our previous articles [2, 6]. Briefly, the fxPET was equipped with dual arc-shaped detectors each covering 135° , with ring diameter of 778 mm and axial extent of 150 mm. The detector block comprises four-layer depth-of-interaction (DOI) crystal blocks of 16×16 arrays of lutetium gadolinium oxyorthosilicate (LGSO) crystal ($2.9 \text{ mm} \times 2.9 \text{ mm} \times 20 \text{ mm}$, Hitachi Chemical, Tokyo, Japan) and a 64-ch MR-compatible silicon photomultiplier array (Hamamatsu Photonics, Hamamatsu, Japan). The coincident resolving time of the TOF detectors is approximately 500 ps full width at half maximum (FWHM). The spatial resolution of these scanners measured with Fluorine-18 point source was estimated to be less than 2.5 mm [2]. For image reconstruction, we used 3D dynamic row-action maximum-likelihood algorithm (3D DRAMA) [2, 7]. We also used corrections with point spread function (PSF) and single scatter simulation (SSS) [8]. The attenuation correction in this investigation was performed using a μ -map obtained by CT as a part of WB PET/CT.

Scanning Protocols of WB PET/CT and fxPET

All patients underwent a WB PET/CT scan approximately 1 h after injection of approximately 200 MBq (mean \pm SD 204.8 ± 37.1 MBq, range 135.7–339.0 MBq) of 2-deoxy-2- ^{18}F fluoro-D-glucose (^{18}F FDG) using a bismuth germanium oxide (BGO)-based PET/CT scanner (Discovery IQ, GE Healthcare, Waukesha, WI, USA) with a crystal dimension of $6.3 \text{ mm} \times 6.3 \text{ mm} \times 30 \text{ mm}$, without time-of-flight (TOF) capability. Specifications of these devices are summarized in Online Resource 1. Our basic protocol for

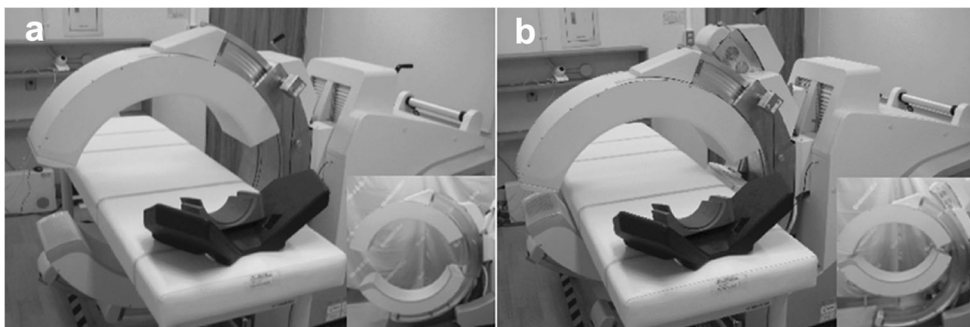


Fig. 1. FxPET scanner with a layout A and b layout B. The detectors were set above and below the patients in layout A, and more closely to the patient in layout B.

Table 1. Disease characteristics ($n = 59$)

Disease	n (%)
Urogenital cancers	10 (16.9 %)
Cancers of gastrointestinal tract	10 (16.9 %)
Lymphoma	10 (16.9 %)
Head and neck cancers	7 (11.9 %)
Lung cancer	6 (10.2 %)
Hepatobiliary cancers	5 (8.5 %)
Pancreatic cancer	4 (6.8 %)
Others	7 (11.9 %)

acquisition time of WB PET/CT was 2 min/bed for patients with body weight (BW) less than 60 kg, and 3 min/bed for patients with body weight more than 60 kg, but the protocol may be modified by the technologist after taking the patient's status into consideration. In this investigation, the basic protocol was applied in 52 of 59 patients, but 2 min/bed was applied in one patient (BW > 60 kg), 2.5 min/bed in two patients (BW > 60 kg), and 3 min/bed in four patients (BW < 60 kg). Patients then underwent fxPET scanning with layout A approximately 90 min after injection, followed by sequential fxPET scanning with layout B. The average duration from the injection to the scanning of WB PET/CT, layout A and layout B in fxPET were 62.9 min (range 52–83 min), 91.4 min (range 71–108 min), and 104.0 min (range 85–119 min), respectively. In fxPET scanning, we scanned only one bed position for each patient; the acquisition time in each fxPET layout was 10 min/bed. The scanner with each layout is demonstrated in Fig. 1. We determined the location for fxPET scanning to include as many lesions as possible with reference to prior PET/CT images. No patients had plasma glucose levels above 200 mg/dL at administration of [^{18}F]FDG.

Image Analysis

Image Quality We analyzed images using Osirix 64bit software (version 8.0.1, Pixmeo, Geneva, Switzerland). To evaluate image quality, two board-certified radiologists and nuclear medicine physicians (YN and TI) rated each image by consensus using a 4-point grading scale (3: perfectly demarcated without distortion, 2: partially mixed with background or faintly distorted, 1: moderately distorted or ill-defined, 0: inappropriate for diagnosis because of degraded image) [9]. We compared the scores for layouts A and B. The representative images of each score are shown in Fig. 2.

Lesion Detectability One board-certified radiologist (MW) identified clinically true positive lesions with reference to pathological findings after biopsy/surgery, and/or radiological findings by comparing lesion size, that is, increase of size during follow-up period. Then, three datasets, *i.e.*, WB PET/CT, layout A, and layout B in fxPET, were simultaneously displayed on a workstation, and lesions with abnormal uptake for which we were able to suspect to be pathological were counted side-by-side. Up to five lesions per organ were chosen for reliable analysis when there were six or more lesions in each organ [9]. Lesions located outside the field of view of fxPET were excluded.

Quantitative Values Lesions that were demarcated and not attached to the adjacent lesions were identified in fxPET images with two layouts and in WB PET/CT images. Volumes of interest (VOIs) were created on each identified lesion and SUVmax was measured. SUVmax was defined as the highest regional uptake in each VOI. The SUVpeak was

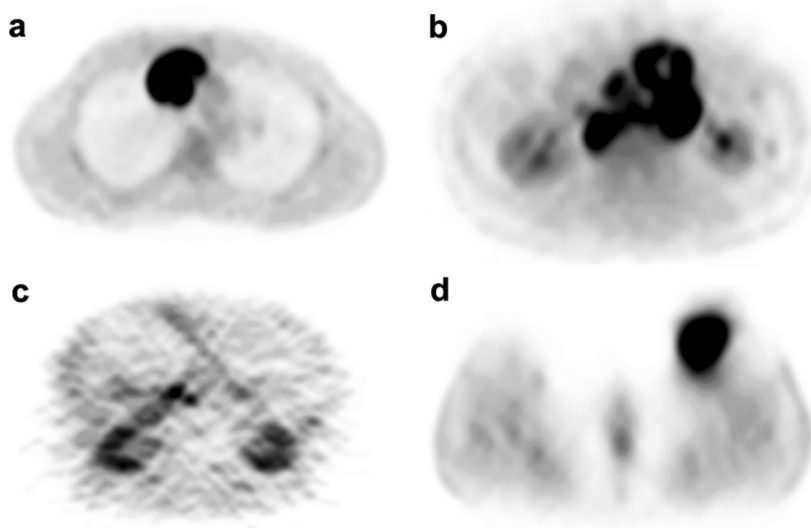


Fig. 2. Four-point grading score for image evaluation. **a** Score 3: perfectly demarcated without distortion; **b** score 2: partially mixed with background or faintly distorted; **c** score 1: moderately distorted or ill-defined; **d** score 0: inappropriate to diagnose due to degraded image.

defined as a maximum average SUV within 1 cm³ spherical volume [10, 11]. The SUV_{peak} was not measured in this evaluation when the minimum diameter of lesions was less than 1.2 cm because it was impossible to fully locate the 1-cm³ VOI sphere within the lesions [10–12]. To determine SUV_{mean}, VOI threshold as 41 % of the lesions' SUV_{max} was used according to the European Association of Nuclear Medicine guidelines 2015 [11]. To determine SUV_{mean}, metabolic tumor volume (MTV) and total lesion glycolysis (TLG), the lesions with accumulation too weak to be delineated clearly in WB PET/CT (or PET as a part of WB PET/CT together with reference enhanced CT/MR) were excluded because we could not accurately separate the tumor from non-tumor tissues because of their physiological uptake. The quantitative values were then compared between the two fxPET layouts and WB PET/CT. In these quantitative analyses, up to five lesions per organ were chosen for reliable analysis as well as the lesion detectability evaluation [9]. Additionally, subanalyses were performed for patients' identified lesions according to the lesion sizes, that is, < 2 cm and ≥ 2 cm. The threshold of the minimal diameter of the lesion (2 cm) was determined by reviewing the previous literature and considering the partial volume effect (PVE) [10, 13, 14]. The sizes of the measurable lesions were basically evaluated using the WB PET/CT CT data (76 lesions in 46 patients). When it was difficult to measure the diameter on low-dose plain CT data of WB PET/CT, corresponding MR or enhanced CT were used to measure the lesion size (26 lesions in 13 patients).

Finally, tumor-to-liver ratio (TLR) and background signal-to-noise ratio (SNR) were calculated and compared according to the previous literature [11, 15, 16]. For these analyses, we took a background region of interest in the normal liver (right hepatic lobe) with a diameter of 3 cm. The TLR was defined as the SUV_{max} of lesions divided by the SUV_{mean} of the background liver. The background SNR was defined as the SUV_{mean} divided by the standard deviation of SUV within the region of interest in the normal liver. These quantitative values were also compared between the two fxPET layouts and WB PET/CT.

Statistical Analysis We used GraphPad Prism version 6 for Windows (GraphPad Software, San Diego, CA, USA) for statistical analyses. A *p* value of less than 0.05 was considered significant for each analysis. We compared the scores between two layouts using Chi-squared test. The lesion detection rates were compared using McNemar's test. The SUV_{max}/mean/peak, MTV and TLG between the fxPET and the WB PET/CT were compared using Spearman's rank correlation coefficient (ρ) and Wilcoxon's signed rank tests. The TLR and background SNR in the two fxPET layouts and those of WB PET/CT were analyzed using Wilcoxon's signed rank tests.

Results

Image Quality

Image quality scores are summarized in Table 2. More cases had score 3 in layout B than in layout A, which is statistically significant ($p < 0.0001$).

Lesion Detectability

Based on final diagnosis, there were 184 clinically true lesions. Of these 184 true lesions, 166 (90.2 %), 169 (91.8 %), and 172 (93.5 %) lesions were depicted by WB PET/CT, and fxPET layouts A and B, respectively. The layout B detection rate was significantly higher than that of WB PET/CT ($p = 0.041$), while there was no significant difference between the layout A and WB PET/CT detection rates. The detection rate of nodal metastases using layout B (91/101, 90.1 %) was significantly higher than using WB PET/CT (85/101, 84.2 %; $p = 0.041$), while the detection rates of other organs in layouts A and B were comparable with that of WB PET/CT (Table 3).

Quantitative Values

Difference and Correlation of SUV_{max}/Mean/Peak, MTV, TLG Between WB PET/CT and fxPET in Each Layout The results of quantitative analyses for all identified lesions are summarized in Tables 4 and 5 and Figs. 3, 4, and 5. The SUV_{max}/mean/peak in all lesions and lesions with minimum diameters less than 2 cm were significantly larger in the two fxPET layouts than in WB PET/CT ($p < 0.01$), while those in lesions equal to or larger than 2 cm in the two fxPET layouts were not significantly different from those in WB PET/CT. The MTVs were significantly lower in the two fxPET layouts than in WB PET/CT ($p < 0.05$), especially in lesions smaller than 2 cm in two layouts ($p < 0.01$). The TLGs of layout B for all lesions and lesions smaller than 2 cm were significantly lower than those of WB PET/CT ($p < 0.01$), while the other TLGs in the two fxPET layouts were comparable with those in WB PET/CT.

All the quantitative values in layouts A and B had significantly strong positive correlations with those in WB PET/CT ($p < 0.0001$). Regarding the subanalyses according to tumor size, all quantitative values in two layouts had also significantly strong positive correlations with WB PET/CT ($p < 0.0001$).

Table 2. The number of cases in each score according to two layouts

Score	Layout A	Layout B
0	0	0
1	4	0
2	53	11
3	2	48

The scores of layout B were significantly better than layout A ($p < 0.0001$)

Table 3. Detectability for each lesion

	WB PET/CT	fxPET	
		Layout A	Layout B
Primary tumors ($n=38$)	37 (97.4 %)	37 (97.4 %)	37 (97.4 %)
Local recurrence ($n=7$)	6 (85.7 %)	6 (85.7 %)	6 (85.7 %)
Nodal mets ($n=101$)	85 (84.2 %)	88 (87.1 %)	91 (90.1 %)*
Liver mets ($n=13$)	13 (100 %)	13 (100 %)	13 (100 %)
Bone mets ($n=12$)	12 (100 %)	12 (100 %)	12 (100 %)
Lung mets ($n=3$)	3 (100 %)	3 (100 %)	3 (100 %)
Peritoneal mets ($n=4$)	4 (100 %)	4 (100 %)	4 (100 %)
Others ($n=6$)	6 (100 %)	6 (100 %)	6 (100 %)
Total ($n=184$)	166 (90.2 %)	169 (91.8 %)	172 (93.5 %)*

* $p=0.041$

Comparison of the TLR and the Background SNR Between WB PET/CT and fxPET The TLRs in WB PET/CT and fxPET (layout A and layout B) were 4.5 ± 1.8 , 5.6 ± 2.0 , and 5.6 ± 2.3 (mean \pm SD), respectively, for 16 hepatic lesions. In fxPET, the TLRs in two layouts were significantly larger than WB PET/CT ($p < 0.0001$; Fig. 6). The background liver SNRs in WB PET/CT and fxPET (layout A and layout B) were 12.5 ± 2.4 , 9.9 ± 2.7 , and 10.8 ± 2.7 (mean \pm SD), respectively in 18 patients. The background SNRs in layouts A and B were significantly lower than in WB PET/CT ($p = 0.0004$, 0.039 , respectively; Fig. 6). The background SNR in layout B was significantly larger than that in layout A ($p = 0.043$).

Discussion

In fxPET scanning, layout B tended to show better image quality ($p < 0.0001$) compared with the conventional layout of detectors

Table 4. Quantitative values obtained by each scanner (mean \pm SD)

	n	WB PET/CT	fxPET	
			Layout A	Layout B
SUVmax				
< 2 cm	76	10.2 ± 6.2	$12.4 \pm 7.6^*$	$12.2 \pm 7.2^*$
≥ 2 cm	26	13.8 ± 6.6	15.5 ± 9.1	14.6 ± 7.8
Total	102	11.1 ± 6.4	$13.2 \pm 8.1^*$	$12.8 \pm 7.4^*$
SUVmean				
< 2 cm	52	7.4 ± 3.8	$9.0 \pm 4.6^*$	$9.0 \pm 4.3^*$
≥ 2 cm	20	9.6 ± 4.4	10.3 ± 5.2	9.9 ± 4.7
Total	72	8.0 ± 4.1	$9.3 \pm 4.8^*$	$9.2 \pm 4.4^*$
SUVpeak				
< 2 cm	44	7.5 ± 4.0	$8.6 \pm 4.6^*$	$8.5 \pm 4.5^*$
≥ 2 cm	26	10.1 ± 5.4	10.6 ± 6.1	10.2 ± 5.1
Total	70	8.5 ± 4.7	$9.3 \pm 5.2^*$	$9.1 \pm 4.8^*$
MTV				
< 2 cm	52	3.7 ± 2.9	$3.1 \pm 2.7^*$	$2.7 \pm 2.4^*$
≥ 2 cm	20	55.4 ± 97.5	$48.0 \pm 84.5^{**}$	$53.5 \pm 100.7^*$
Total	72	18.1 ± 55.6	$15.5 \pm 48.2^*$	$16.8 \pm 56.9^*$
TLG				
< 2 cm	52	29.2 ± 32.6	28.7 ± 31.7	$25.9 \pm 28.4^*$
≥ 2 cm	20	555.2 ± 913.7	504.8 ± 840.9	560.1 ± 1013.0
Total	72	175.3 ± 529.6	160.9 ± 485.9	$174.3 \pm 577.4^*$

fxPET flexible PET, SUV standardized uptake value, MTV metabolic tumor volume, TLG total lesion glycolysis

* $p < 0.01$, ** $p < 0.05$,

(layout A), and comparable or higher detection rate was obtained compared with WB PET/CT and fxPET layout A. The SUVmax/mean/peak in lesions smaller than 2 cm in the two fxPET layouts were significantly larger than those in WB PET/CT ($p < 0.01$). The MTVs in the two fxPET layouts were significantly lower than in WB PET/CT ($p < 0.05$), especially in lesions smaller than 2 cm ($p < 0.01$). The TLG in the two fxPET layouts tended to be comparable with that in WB PET/CT, except in the total lesions and lesions smaller than 2 cm in layout B ($p < 0.01$). Concerning the correlation analyses of the quantitative values, including subanalyses according to tumor size, all quantitative values of fxPET had significantly strong positive correlations with WB PET/CT ($p < 0.0001$). The TLRs in the two fxPET layouts were significantly larger than those in WB PET/CT ($p < 0.0001$). Additionally, the background SNR was significantly larger in layout B than in layout A ($p < 0.05$), but it was significantly lower compared with WB PET/CT ($p < 0.05$).

As to the image quality of fxPET, the score was 2 in most cases in layout A, but it was 3 in more than 80 % of cases in layout B, which indicates comparable quality with WB PET/CT, as was expected. In layout A, some detectors were missing in part of the gantry, which caused degradation of image quality because of the incomplete coincident data. In layout B, putting detectors closer to patients meant that there were no gaps, like in full-ring type PET scanners. Additionally, TOF and PSF algorithms as well as the longer acquisition time in fxPET, *i.e.*, 10 min/bed in fxPET vs. 2–3 min/bed in WB PET/CT, might have contributed to the good image quality [3, 17–20], although fxPET scanning was performed after WB PET/CT scanning, which resulted in reduction of photons owing to the relatively short half-life of fluorine-18 [21]. The fxPET scanners employed four-layer DOI detectors, which might be one of the reasons that layout B outperformed layout A in many of the performance measures; the four-layer DOI detector arrangement suppresses parallax error, especially near the detector arc, which is the main imaging area of layout B [22, 23].

We showed the good detectability of fxPET, but it can be claimed that 10-min scans with fxPET at 90 min postinjection resulted in diagnostic quality images, albeit for limited axial field of view. In this investigation, we applied a 10-min

Table 5. Correlations of quantitative values (Spearman's rho)

	<i>n</i>	Layout A	Layout B
SUVmax			
< 2 cm	76	0.93	0.92
≥ 2 cm	26	0.89	0.90
Total	102	0.93	0.93
SUVmean			
< 2 cm	52	0.89	0.88
≥ 2 cm	20	0.90	0.84
Total	72	0.90	0.88
SUVpeak			
< 2 cm	44	0.96	0.94
≥ 2 cm	26	0.93	0.90
Total	70	0.94	0.93
MTV			
< 2 cm	52	0.91	0.88
≥ 2 cm	20	0.96	0.99
Total	72	0.95	0.94
TLG			
< 2 cm	52	0.97	0.97
≥ 2 cm	20	0.98	0.99
Total	72	0.98	0.98

SUV standardized uptake value, MTV metabolic tumor volume, TLG total lesion glycolysis

All *p* values in two layouts of fxPET were <0.0001

acquisition time in fxPET scanning only because it had been applied in our previous study [2]. We also compared fxPET images with PET images obtained by conventional PET/CT in clinical settings. Because this is not considered a fair comparison between WB PET/CT and fxPET, at this time, we do not conclude that the detectability of fxPET is superior to that of WB PET/CT because the longer uptake phase would contribute to higher tumor-to-background ratios in PET using [¹⁸F]FDG [24]. Therefore, for a fair

comparison, we need to evaluate the detectability under the same conditions, after determining the optimal scanning time of fxPET. In addition, to alleviate the bias caused by delayed imaging, half of the patients should be imaged by the fxPET prior to WB PET/CT imaging and the remaining half of the patients should be imaged by the fxPET afterwards.

The quantitative values including SUVmax/mean/peak, MTV, and TLG in the two fxPET layouts had significant strong positive correlations with WB PET/CT (*p* < 0.0001). The SUVmax/mean/peak in two layouts tended to be larger than those in WB PET/CT, while the MTVs in the two fxPET layouts tended to be lower than those in WB PET/CT. The TLGs in the two fxPET layouts tended to be comparable with those in WB PET/CT. The reason for larger SUVmax/mean/peak in fxPET than in WB PET/CT are considered to mainly be the higher spatial resolution of fxPET [2, 14, 18] as well as faster convergence owing to TOF, especially for smaller lesions [19, 25]. The longer duration between administration of [¹⁸F]FDG and starting time of acquisition may also have been a partial contributor [24]; the average scanning time intervals of WB PET/CT, first and second scanning of fxPET from the injection were 62.9 min, 91.4 min, and 104.0 min, respectively. Generally, the SUVmax of malignant tumors increases even more than 1 h after the injection [24]. Considering the similar pixel sizes of the Discovery IQ (3.1 mm) and fxPET (3.0 mm), the effect of the different pixel sizes may be minimum. The higher SUVmax in fxPET may cause a smaller MTV than those in WB PET/CT. The comparable TLGs in fxPET with those in WB PET/CT may be influenced by both the larger SUVmean and the smaller MTV of fxPET. In the subanalyses, the SUVmax/mean/peak of lesions smaller than

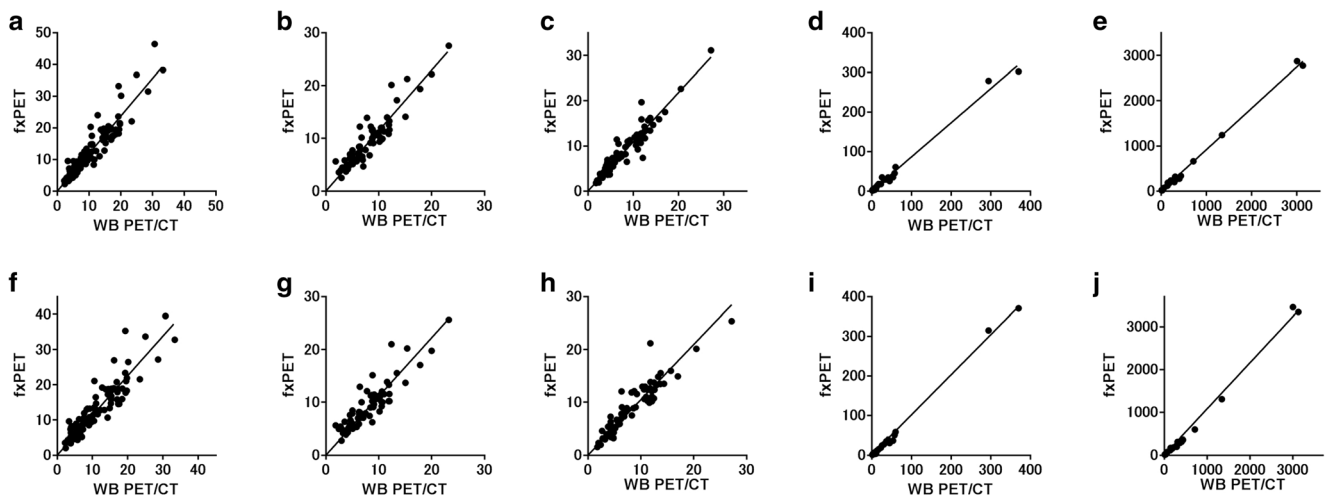


Fig. 3. Correlation of quantitative values between whole-body (WB) PET/CT and flexible PET (fxPET) in each layout (**a–e** layout A; **f–j** layout B). There were 102, 72, 70, 72, and 72 lesions in the analyses of **a, f** SUVmax (standardized uptake value); **b, g** SUVmean; **c, h** SUVpeak; **d, i** MTV (metabolic tumor volume), and **e, j** TLG (total lesion glycolysis), respectively (*p* < 0.0001). **a** $y = 1.18x$; **b** $y = 1.15x$; **c** $y = 1.09x$; **d** $y = 0.86x$; **e** $y = 0.92x$; **f** $y = 1.13x$; **g** $y = 1.11x$; **h** $y = 1.05x$; **i** $y = 1.01x$; **j** $y = 1.08x$.

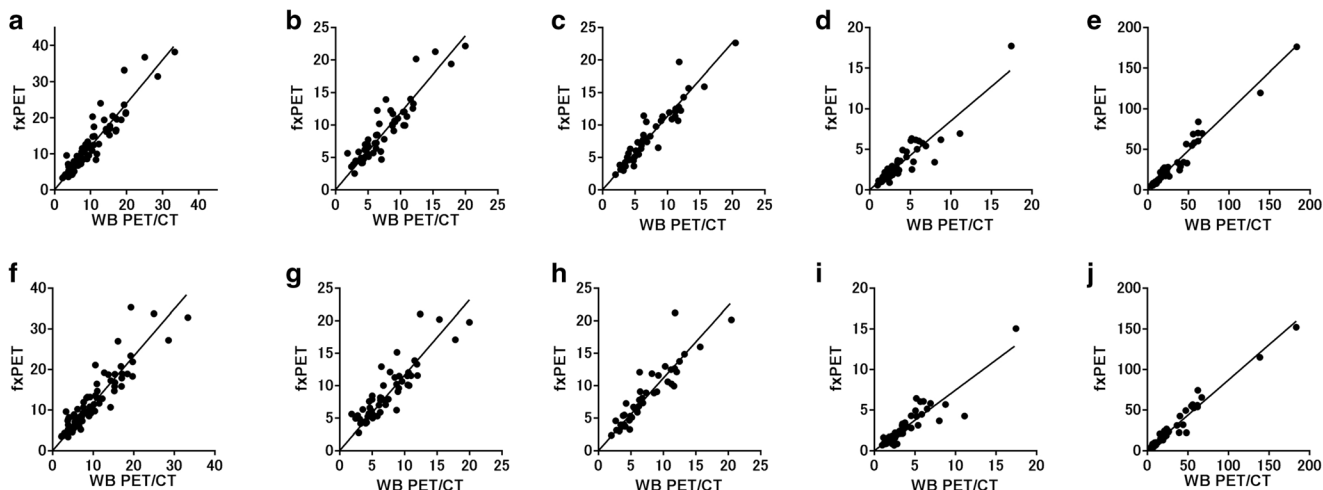


Fig. 4. Correlation of quantitative values between whole-body (WB) PET/CT and flexible PET (fxPET) in the lesions smaller than 2 cm (**a–e** layout A; **f–j** layout B). There were 76, 52, 44, 52, and 52 lesions in the analyses of **a, f** SUVmax (standardized uptake value); **b, g** SUVmean; **c, h** SUVpeak; **d, i** MTV (metabolic tumor volume); and **e, j** TLG (total lesion glycolysis), respectively ($p < 0.0001$). **a** $y = 1.20x$; **b** $y = 1.18x$; **c** $y = 1.13x$; **d** $y = 0.85x$; **e** $y = 0.97x$; **f** $y = 1.16x$; **g** $y = 1.16x$; **h** $y = 1.11x$; **i** $y = 0.74x$; **j** $y = 0.87x$.

2 cm in the two fxPET layouts tended to be significantly much larger than in WB PET/CT compared with the results of lesions equal or larger than 2 cm in fxPET. This may be because of the advantage of TOF algorithm of fxPET over WB PET/CT, which enables good contrast recovery for spheres 2 cm or smaller and the mitigation of the PVE in small lesions of fxPET [19, 25].

The TLRs in the two fxPET layouts were significantly larger than in WB PET/CT, which is likely due to the delayed scan time [24, 26, 27]. According to the previous literature, the SUVmax of malignant tumors increases over time and plateaus around 2 h after the injection [24, 27]. The SUVmean of the background liver was expected to be nearly constant between 50 and 110 min after the injection [26].

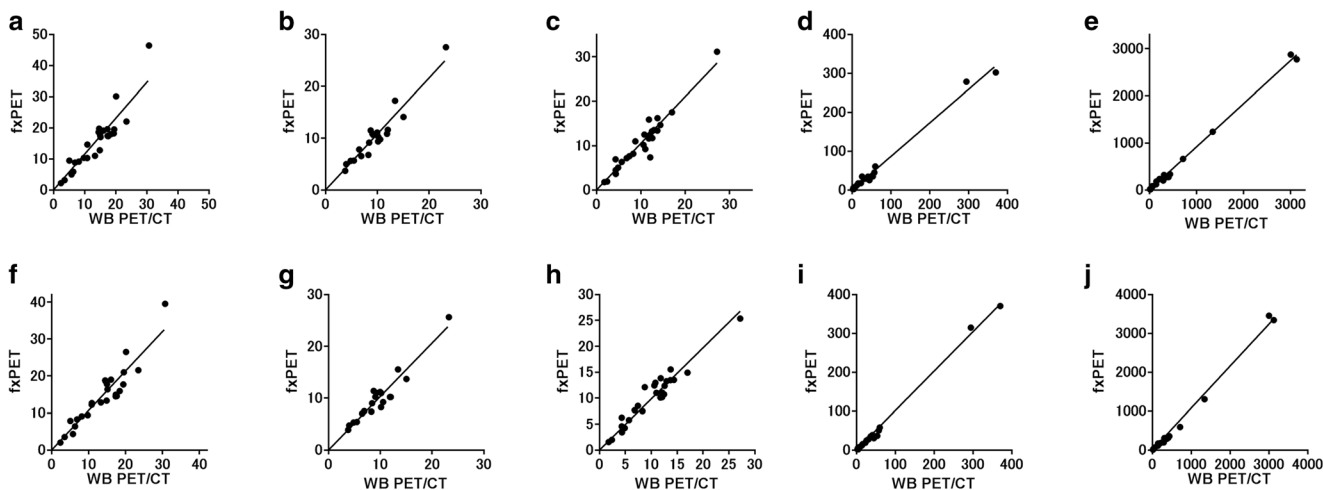


Fig. 5. Correlation of quantitative values between whole-body (WB) PET/CT and flexible PET (fxPET) in the lesions equal or larger than 2 cm (**a–e** layout A; **f–j** layout B). There were 26, 20, 26, 20, and 20 lesions in the analyses of **a, f** SUVmax (standardized uptake value); **b, g** SUVmean; **c, h** SUVpeak; **d, i** MTV (metabolic tumor volume); and **e, j** TLG (total lesion glycolysis), respectively ($p < 0.0001$). **a** $y = 1.15x$; **b** $y = 1.08x$; **c** $y = 1.05x$; **d** $y = 0.86x$; **e** $y = 0.92x$; **f** $y = 1.07x$; **g** $y = 1.03x$; **h** $y = 0.99x$; **i** $y = 1.01x$; **j** $y = 1.08x$.

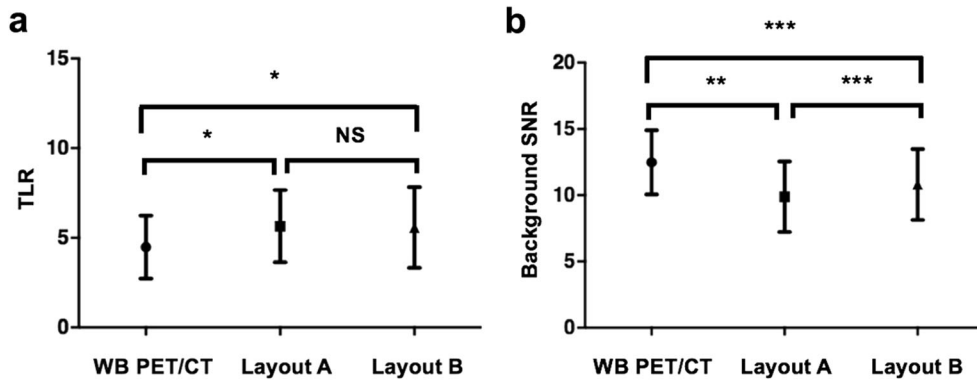


Fig. 6. Comparison of tumor-to-liver ratio (**a** TLR) and background signal-to-noise ratio (**b** SNR) between whole-body (WB) PET/CT and flexible PET (fxPET) in each layout (mean \pm SD). **a** The TLRs in fxPET tended to be larger than WB PET/CT, although there was no statistically significant difference between the two layouts (* $p < 0.0001$, NS: not significant). **b** The background SNRs in fxPET tended to be lower than WB PET/CT, especially in layout A (** $p < 0.0005$, *** $p < 0.05$).

For this reason, it is reasonable to obtain higher TLRs in fxPET. However, the background SNR of fxPET, especially in layout A, was significantly lower than in WB PET/CT. This may be because of the incomplete partial-ring detectors, as was seen in our previous study, or the dedicated-breast PET system [3, 28]. The scanning with the partial-ring detectors reduces sensitivity because of the loss of counts in the missing lines-of-responses (LORs), and we must mitigate the disadvantages by TOF reconstruction [28]. In layout B, in which detectors were set more closely, the background SNR was significantly improved compared with that of layout A ($p < 0.05$), which demonstrates the quantitative advantages of layout B over Layout A.

There are some limitations to our study. First, the sample size may be small. Second, we were unable to obtain pathological confirmation of all lesions because of an ethical issue. Third, there was a substantial difference in the scan range and scan duration between fxPET and WB PET/CT; the scan range of fxPET in the axial direction was limited to only one bed position (axial FOV, 150 mm), and the acquisition times per one bed of WB PET/CT and fxPET were 2–3 min and 10 min, respectively, because WB PET/CT was performed as a routine clinical study, and the acquisition time of fxPET was longer, based on our previous preliminary work. Therefore, for a fair and exact comparison between the two scanners, further evaluations are necessary.

Conclusion

The fxPET system yielded reasonable image quality and quantitative accuracy, compared with those of the conventional BGO-based WB PET/CT scanner without TOF capability. Bringing the detectors closer to the patients yielded improved results. To assess the optimal scanning time in fxPET, and to compare the diagnostic performance of this scanner with the current WB PET/CT scanner more properly, further investigations are required.

Acknowledgments. We thank Yoshiyuki Yamakawa, Masafumi Furuta, Masanobu Satoh, Tetsuya Kobayashi, Junichi Ohi, and Keishi Kitamura for their technical advice.

Compliance with Ethical Standards

Conflict of Interest

This prototype fxPET was manufactured by Shimadzu Corporation, Kyoto, Japan. This study was based on results obtained from a project commissioned by the New Energy and Industrial Technology Development Organization (NEDO). This study was also supported by The Kyoto University Foundation (Public Interest Incorporated Foundation, the support for attending symposia). No other potential conflicts of interest relevant to this article exist.

Ethical Approval

All procedures performed in studies involving human participants were in accordance with the ethical standards of the institutional and/or national research committee and with the 1964 Helsinki declaration and its later amendments or comparable ethical standards.

Informed Consent

Informed consent was obtained from all individual participants included in the study.

References

1. Nensa F, Beiderwellen K, Heusch P, Wetter A (2014) Clinical applications of PET/MRI: current status and future perspectives. *Diagn Interv Radiol* 20:438–447
2. Nakamoto R, Nakamoto Y, Ishimori T, Fushimi Y, Kido A, Togashi K (2018) Comparison of PET/CT with sequential PET/MRI using an MRI-compatible mobile PET system. *J Nucl Med* 59:846–851
3. Kobayashi T, Kitamura K (2012) Design considerations for a partial-ring, multi-modal compatible whole-body TOF PET scanner: flexible PET. in *Conf Rec IEEE NSS/MIC 2807–2812*
4. Nakazawa M, Ohi J, Furumiya T, et al. (2012) PET data acquisition (DAQ) system having scalability for the number of detector. in *Conf Rec IEEE NSS/MIC 2475–2478*
5. Furuta M, Satoh M, Ohi J, et al. (2013) Development of a proof of concept system for multi-modal compatible PET: flexible PET. in *Conf. Rec. IEEE NSS/MIC 1–4*
6. Yamakawa Y, Kobayashi T, Furuta M, et al. (2014) Development of a dual-head mobile DOI-TOF PET system having multi-modality compatibility. in *Conf. Rec. IEEE NSS/MIC 1–3*

7. Tanaka E, Kudo H (2010) Optimal relaxation parameters of DRAMA (dynamic RAMLA) aiming at one pass image reconstruction for 3D PET. *Phys Med Biol* 55:2917–2939
8. Watson CC (2007) Extension of single scatter simulation to scatter correlation of time-of-flight PET. *IEEE Trans on Nucl Sci* 54:1679–1686
9. Drzewga A, Souvatzoglou M, Eiber M, Beer AJ, Furst S, Martinez-Moller A, Nekolla SG, Ziegler S, Ganter C, Rummeny EJ, Schwaiger M (2012) First clinical experience with integrated whole-body PET/MR: comparison to PET/CT in patients with oncologic diagnoses. *J Nucl Med* 53:845–855
10. Wahl RL, Jacene H, Kasamon Y, Lodge MA (2009) From RECIST to PERCIST: evolving considerations for PET response criteria in solid tumors. *J Nucl Med* 50(Suppl 1):122S–150S
11. Boellaard R, Delgado-Bolton R, Oyen WJ, Giammarile F, Tatsch K, Eschner W, Verzijlbergen FJ, Barrington SF, Pike LC, Weber WA, Stroobants S, Delbeke D, Donohoe KJ, Holbrook S, Graham MM, Testanera G, Hoekstra OS, Zijlstra J, Visser E, Hoekstra CJ, Pruim J, Willemsen A, Arends B, Kotzerke J, Bockisch A, Beyer T, Chiti A, Krause BJ, European Association of Nuclear Medicine (EANM) (2015) FDG PET/CT: EANM procedure guidelines for tumour imaging: version 2.0. *Eur J Nucl Med Mol Imaging* 42:328–354
12. Murphy JD, Chisholm KM, Daly ME, Wiegner EA, Truong D, Iagaru A, Maxim PG, Loo BW Jr, Graves EE, Kaplan MJ, Kong C, le QT (2011) Correlation between metabolic tumor volume and pathologic tumor volume in squamous cell carcinoma of oral cavity. *Radiother Oncol* 101:356–361
13. Schwartz LH, Bogaerts J, Ford R, Shankar L, Therasse P, Gwyther S, Eisenhauer EA (2009) Evaluation of lymph nodes with RECIST 1.1. *Eur J Cancer* 45:261–267
14. Soret M, Bacharach SL, Buvat I (2007) Partial-volume effect in PET tumor imaging. *J Nucl Med* 48:932–945
15. Parvizi N, Franklin JM, McGowan DR et al (2015) Does a novel penalized likelihood reconstruction of ^{18}F -FDG PET-CT improve signal-to-background in colorectal liver metastases? *Eur J Radiol* 84:1873–1878
16. Teoh EJ, McGowan DR, Bradley KM et al (2016) Novel penalised likelihood reconstruction of PET in the assessment of histologically verified small pulmonary nodules. *Eur Radiol* 26:576–584
17. van der Vos CS, Koopman D, Rijnsdorp S, Arends AJ, Boellaard R, van Dalen J, Lubberink M, Willemsen ATM, Visser EP (2017) Quantification, improvement, and harmonization of small lesion detection with state-of-art PET. *Eur J Nucl Med Mol Imaging* 44(Suppl 1):4–16
18. Surti S, Karp JS (2016) Advances in time-of-flight PET. *Phys Med* 32:12–22
19. Conti M (2011) Focus on time-of-flight PET: the benefits of improved time resolution. *Eur J Nucl Med Mol Imaging* 38:1147–1157
20. Kadrmas DJ, Casey ME, Conti M, Jakoby BW, Lois C, Townsend DW (2009) Impact of time-of-flight on PET tumor detection. *J Nucl Med* 50:1315–1323
21. Laffon E, Barret O, Marthan R, Ducassou D (2009) Is the physical decay correction of the ^{18}F -FDG input function in dynamic PET imaging justified? *J Nucl Med Technol* 37:111–113
22. Schmall JP, Karp JS, Werner M, Surti S (2016) Parallax error in long-axial field-of-view PET scanners—a simulation study. *Phys Med Biol* 61:5443–5455
23. Nakazawa M, Ohi J, Tonami H, et al. (2010) Development of a prototype DOI-TOF-PET scanner. in *Conf. Rec. IEEE NSS/MIC* 2077-2080
24. Kubota K, Itoh M, Ozaki K, Ono S, Tashiro M, Yamaguchi K, Akaizawa T, Yamada K, Fukuda H (2001) Advantage of delayed whole-body FDG-PET imaging for tumour detection. *Eur J Nucl Med* 28:696–703
25. Murray I, Kalemis A, Glennon J, Hasan S, Quraishi S, Beyer T, Avril N (2010) Time-of-flight PET/CT using low-activity protocols: potential implications for cancer therapy monitoring. *Eur J Nucl Med Mol Imaging* 37:1643–1653
26. Laffon E, Adhoute X, de Clermont H, Marthan R (2011) Is liver SUV stable over time in ^{18}F -FDG PET imaging? *J Nucl Med Technol* 39:258–263
27. Al-Faham Z, Jolepalem P, Rydberg J et al (2016) Optimizing ^{18}F -FDG uptake time before imaging improves the accuracy of PET/CT in liver lesions. *J Nucl Med Technol* 44:70–72
28. Surti S, Karp JS (2008) Design considerations for a limited angle, dedicated breast, TOF PET scanner. *Phys Med Biol* 53:2911–2921

Publisher’s Note Springer Nature remains neutral with regard to jurisdictional claims in published maps and institutional affiliations.